frontiers | Frontiers in Chemistry

ORIGINAL RESEARCH
published: 03 June 2022
doi: 10.3389/fchem.2022.900962

Electrocatalytic Reduction of Nitrate *via* Co_3O_4/Ti Cathode Prepared by Electrodeposition Paired With IrO_2-RuO_2 Anode

Chuan Wang[1], *Zhifen Cao*[1], *Hongtao Huang*[1], *Hong Liu*[2] *and Sha Wang*[2]*

[1]Key Laboratory for Water Quality and Conservation of the Pearl River Delta, Ministry of Education, Institute of Environmental Research at Greater Bay, Guangzhou University, Guangzhou, China, [2]Chongqing Institute of Green and Intelligent Technology, Chinese Academy of Sciences, Chongqing, China

Nitrate pollution is already a global problem, and the electrocatalytic reduction of nitrate is a promising technology for the remediation of wastewater and polluted water bodies. In this work, Co_3O_4/Ti electrodes were prepared by electrodeposition for the electrocatalytic reduction of nitrate. The morphology, chemical, and crystal structures of Co_3O_4/Ti and its catalytic activity were investigated. Then, the electrocatalytic nitrate reduction performance of Co_3O_4/Ti as the cathode was evaluated by monitoring the removal efficiencies of nitrate (NO_3^--N) and total nitrogen (TN), generation of reduction products, current efficiency (CE), and energy consumption (EC) at different operating conditions. Under the catalysis of Co_3O_4/Ti, NO_3^- was reduced to N_2 and NH_4^+, while no NO_2^- was produced. After the introduction of chloride ions and IrO_2-RuO_2/Ti as the anode, NH_4^+ was selectively oxidized to N_2. The removal efficiencies of NO_3^--N (at 100 mg/L) and TN after 2 h were 91.12% and 60.25%, respectively (pH 7.0; Cl^- concentration, 2000 mg/L; current density, 15 mA/cm^2). After 4 h of operation, NO_3^--N and TN were completely removed. However, considering the EC and CE, a 2-h reaction was the most appropriate. The EC and CE were 0.10 kWh/g NO_3^-N and 40.3%, respectively, and electrocatalytic performance was maintained after 10 consecutive reduction cycles (2 h each). The cathode Co_3O_4/Ti, which is prepared by electrodeposition, can effectively remove NO_3^--N, with low EC and high CE.

Keywords: nitrate removal, electrocatalytic, Co_3O_4/Ti, reduction, IrO_2-RuO_2

OPEN ACCESS

Edited by:
Qingyi Zeng,
University of South China, China

Reviewed by:
Huawei Song,
Sun Yat-sen University, China
Qing Lan,
Guangdong Polytechnic of Environmental Protection Engineering, China

***Correspondence:**
Sha Wang
wangsha@cigit.ac.cn

Specialty section:
This article was submitted to Inorganic Chemistry, a section of the journal Frontiers in Chemistry

Received: *21 March 2022*
Accepted: *19 April 2022*
Published: *03 June 2022*

Citation:
Wang C, Cao Z, Huang H, Liu H and Wang S (2022) Electrocatalytic Reduction of Nitrate via Co_3O_4/Ti Cathode Prepared by Electrodeposition Paired With IrO_2-RuO_2 Anode. Front. Chem. 10:900962. doi: 10.3389/fchem.2022.900962

1 INTRODUCTION

Nitrate (NO_3^-) contamination of surface water and groundwater is a global environmental problem associated with increasing populations, and its hazards have attracted much attention (Jasper et al., 2014; Khalil et al., 2016; Serio et al., 2018). The accumulation of plant nutrients such as NO_3^- and phosphate in water can accelerate eutrophication, a process that increases the biomass of a water body as its biological diversity decreases, for example, due to increases in invertebrates and fish. In the extreme, a state of hypoxia can exist, resulting in the loss of the aquatic ecosystems (Kubicz et al., 2018; Zhang et al., 2021). Although NO_3^- is chemically stable, it can be microbially reduced to reactive nitrite in the oral cavity and stomach, which has been linked to liver damage, methemoglobinemia, and cancer in animals (Spalding and Exner, 1993; Elmidaoui et al., 2001; Barakat et al., 2020).

Currently, microbial denitrification is widely used for the large-scale remediation of NO_3^- pollution (Clauwaert et al., 2007; Della Rocca and Belgiorno V Meriç, 2007). Many other methods of NO_3^- removal have been explored such as reverse osmosis, ion exchange, ammonia stripping, electrodialysis, catalytic reduction, and electrocatalytic reduction (Kapoor and Viraraghavan, 1997; Yang and Lee, 2005; Della Rocca and Belgiorno V Meriç, 2007). Among these techniques, the electrocatalytic reduction of NO_3^- is a promising and clean technology because the electron reductants neither introduce pollutants nor adversely affect the environment (Garcia-Segura et al., 2018; Gayen et al., 2018).

The mechanism of the electrochemical NO_3^- reduction reaction (NO_3^--RR) involves anodic oxidation and cathodic reduction in which NO_3^- is reduced to NO_2^-, NH_4^+, and N_2 on the active sites of the cathode according to **Eqs 1–3** (Zhang et al., 2021):

$$NO_3^- + 2e^- + H_2O \rightarrow NO_2^- + 2OH^-, \quad (1)$$

$$NO_2^- + 6e^- + 6H_2O \rightarrow NH_4^+ + 8OH^-, \quad (2)$$

$$2NO_3^- + 10e^- + 6H_2O \rightarrow N_2 + 12OH^-. \quad (3)$$

The choice of the cathode material is important in this process. To date, most studies have used high-cost noble metal cathodes, such as Pt, Rh, and Pd, which may limit their commercial application (Taguchi and Feliu, 2007; Yang et al., 2014; Soto-Hernández et al., 2019). Co_3O_4 is a cost-effective catalyst, and the preparation of a CuO-Co_3O_4/Ti electrode by the sol-gel method for electrochemical reduction of NO_3^- was recently reported (Yang et al., 2020). The system demonstrated the complete removal of NO_3^- after 3 h at a current density of 20 mA/cm^2.

NO_2^- and NH_4^+ generated at the cathode (**Eqs. (1)** and **(2)**) diffuse to the anode where they are adsorbed onto the surface and subsequently oxidized to NO_3^- and N_2 (**Eqs. (4)** and **(5)**) (Zhang et al., 2021):

$$NO_2^- + H_2O \rightarrow NO_3^- + 2e^- + 2H^+, \quad (4)$$

$$2NH_4^+ \rightarrow N_2 + 6e^- + 6H^+. \quad (5)$$

When Cl^- is present in the electrolyte, the following reactions also occur at the anode (**Eqs. 6–9**) (Zhang et al., 2021):

$$2Cl^- \rightarrow Cl_2 + 2e^-, \quad (6)$$

$$Cl_2 + H_2O \rightarrow HOCl + Cl^- + H^+, \quad (7)$$

$$HOCl \rightarrow ClO^- + H^+, \quad (8)$$

$$2NH_4^+ + 3ClO^- \rightarrow N_2 + 3H_2O + 2H^+ + 3Cl^-. \quad (9)$$

The electrochemical NO_3^--RR involves NO_3^- reduction at the cathode and ammonium nitrogen (NH_4^+-N) oxidation at the anode. Cl_2 generated at the anode (**Eq. (6)**) immediately forms hypochlorite (**Eq. (7)**), which selectively oxidizes NH_4^+ to N_2 (Su et al., 2017). Hence, the efficient anodic oxidation of chloride ions is a key requirement for this process, and the anode materials used in the chlor-alkali industry, which obtain Cl_2 by electrolysis of sodium chloride, provide a useful reference (Yi et al., 2007). Among these materials, IrO_2-RuO_2 is a good choice due to its low overpotential, high chlorine selectivity, and long-term stability (Chen et al., 2007). In addition, the electrocatalytic reduction of NO_3^--N is also affected by reaction potential, current, solution pH, battery structure, and anode material.

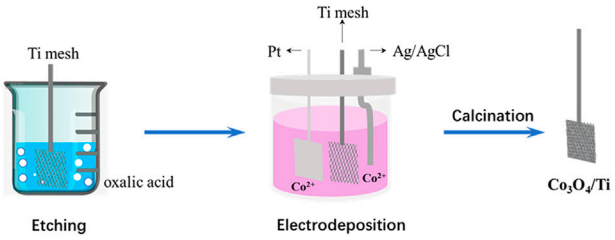

FIGURE 1 | Schematic of the preparation procedure.

Here, a catalytic cathode was prepared by the *in situ* electrodeposition of Co_3O_4 on a titanium substrate (Co_3O_4/Ti) to obtain improved electrocatalytic performance. IrO_2-RuO_2/Ti was employed as the anode for the effective removal of NH_4^+-N and TN. The aim of this study was to obtain simultaneous electrochemical NO_3^- reduction and oxidation of the *in situ*-generated NO_2^- and NH_4^+ into N_2 gas. The morphology and structure of Co_3O_4/Ti were characterized using conventional methods, and its performance in NO_3^- removal was evaluated under different operating conditions. The current efficiency (CE) and energy consumption (EC) of the system were also measured to assess its commercial application.

2 EXPERIMENTAL SECTION

2.1 Chemicals and Materials

The Ti mesh and Ti plate (99.5% purity, 0.6 mm, 10 mesh) were purchased from Lanruiyinde Electrochemical Materials Co., Ltd. (China). The Pt plate was obtained from Aidahengsheng Co., Ltd., (Tianjin, China). All chemicals were of analytical grade. Potassium nitrate and sodium hydroxide were purchased from Aladdin Biochemical Technology Co., Ltd. (Shanghai, China). Cobalt nitrate hexahydrate, sodium eicosyl, hexachloroiridic acid, and ruthenium (III) chloride were obtained from Macklin Biochemical Technology Co., Ltd. (Shanghai, China). Solutions were prepared using deionized water (>15 MΩ cm) obtained from an Elix® 3 purification system (Millipore, United States). Simulated wastewater was prepared by adding potassium nitrate to deionized water.

2.2 Preparation of Co_3O_4/Ti Cathode and IrO_2-RuO_2/Ti Anode

Samples of the Ti mesh and Ti plate (3 × 4 cm, 12 cm^2) were degreased with NaOH solution (40 wt%) at 95°C for 2 h before etching by boiling in oxalic acid solution (10 wt%) for 2 h. The treated samples were then rinsed with deionized water and stored in ethanol until further use.

As shown in **Figure 1**, the Co_3O_4/Ti electrode was prepared using an electrodeposition method. A three-electrode system was employed in a single compartment cell using the pretreated Ti mesh as the cathode, the Pt plate as the anode, and an Ag/AgCl

reference electrode. The electrodeposition solution comprised boric acid (0.5 M), cobalt nitrate hexahydrate (0.1 M), and sodium eicosyl sulfonate (2.0 g/L). Following electrodeposition at a current of 0.25 A for 5 min, the electrode was cleaned with deionized water and oven-dried (60°C) before heating at 5°C/min to 500°C (hold 2 h) in a muffle furnace to effect calcination. The treated samples were allowed to cool naturally to room temperature.

The IrO_2-RuO_2/Ti anode was prepared by using a thermal decomposition method. A mixed solution of hexachloroiridic acid and ruthenium (III) chloride in n-butanol (molar ratio, 2:1) was evenly coated onto the surfaces of the pretreated titanium plate, dried at 105°C for 10 min, and then calcined at 500°C for 15 min. The process was repeated until the weight of the titanium plate increased by about 10 g/cm^2. Finally, the electrode was washed with deionized water before use.

2.3 Characterization of the Co_3O_4/Ti Cathode

Surface morphology and elemental composition were studied by field-emission scanning electron microscopy (SEM) and energy-dispersive X-ray spectroscopy (EDS) on a Phenom ProX system (Thermo Fisher Scientific, United States) at an accelerating voltage of 15 kV. The crystal structure of Co_3O_4 was examined by X-ray diffraction (XRD) with an X'pert Powder system (Malvern Panalytical, Malvern, UK) using Cu Kα (λ = 1.5406 Å) irradiation.

2.4 Electrochemical Measurements

NO_3^--RR tests were performed in a single chamber electrolytic cell (200 ml) using a three-electrode system, with Co_3O_4/Ti (or Ti as required), Pt plate, and Ag/AgCl as the working, counter, and reference electrodes, respectively. The electrolyte was prepared using Na_2SO_4 (0.1 M) and different concentrations of NO_3^--N (KNO_3) as required. Linear sweep voltammetry (LSV), and electrolysis tests were performed in an electrochemical workstation (Metrohm Autolab M204, Switzerland). Prior to the electrochemical test, oxygen was removed by bubbling high-purity N_2 through the electrolyte for ≥20 min, and continuously fed during the experiments.

Electrolysis measurements were performed at an optimum current density of 15 mA/cm^2, and aliquots of the reaction solutions (2 ml) were removed at predetermined time intervals to measure the concentrations of NO_3^--N, NO_2^--N, and NH_4^+-N. The effects of chlorine on NO_3^--RR and the stability of the Co_3O_4/Ti cathode electrode were assessed at a current density of 15 mA/cm^2 for 2 h and an initial NO_3^--N concentration of 100 mg/L.

2.5 Analytical Methods

During the NO_3^--RR, the formation of NO, N_2O, and NH_3 are negligible, and hence, the generated gaseous products can be considered as N_2 (Teng et al., 2018). UV-Vis spectroscopy was used to measure the concentrations of NO_3^--N, NO_2^--N, NH_4^+-N, and total nitrogen (TN) (Evolution 201, Thermofisher Scientific Co., Ltd.), and their removal efficiencies were calculated according to **Eqs (10)–(12)**:

$$NO_3^- - N\ removal = \frac{C_0\left(NO_3^- - N\right) - C_t\left(NO_3^- - N\right)}{C_0\left(NO_3^- - N\right)} \times 100\%, \tag{10}$$

$$NH_4^+ - N\ generation = \frac{C_t\left(NH_4^+ - N\right)}{C_0\left(NO_3^- - N\right)} \times 100\%, \tag{11}$$

$$TN\ removal = \frac{C_0\left(TN\right) - C_t\left(TN\right)}{C_0\left(TN\right)} \times 100\%, \tag{12}$$

where C_0(NO_3^--N) (mg/L) is the initial concentration of NO_3^--N, C_t(NO_3^--N) (mg/L) is the concentration of NO_3^--N at time t, C_t(NH_4^+-N) (mg/L) is the concentration of NH_4^+-N at time t, C_0(TN) (mg/L) is the initial concentration of TN, and C_t(TN) (mg/L) is the concentration of TN at time t.

EC was calculated using **Eq. 13** (Zhang et al., 2016):

$$\mathrm{EC} = \frac{\mathrm{UIt}}{\mathrm{V}\left(\mathrm{C_0} - \mathrm{C_t}\right)}, \tag{13}$$

where U is the cell potential (V), I is the current (A), t is the reaction time (h), and V is the volume of reaction solution (L).

The CE for TN removal rates was obtained using **Eq. 14**:

$$\mathrm{CE}\,(\%) = \frac{(\mathrm{C_0} - \mathrm{C_t}) \times \mathrm{V}}{\mathrm{M} \times \mathrm{Q}} \times \mathrm{n} \times 96485 \times 100\%, \tag{14}$$

where M is the molar mass of N (14 g/mol), Q is the amount of electricity passing through the electrode, and n is the number of electrons obtained from the complete reduction of NO_3^--N (calculated according to the conversion of NO_3^- to N, n = 5).

3 RESULTS AND DISCUSSION

3.1 Electrode Characterizations and Chemical Tests

SEM was used to depict the electrode surface morphology of Co_3O_4/Ti. **Figure 2** shows that spherical particles (3–5 μm) of Co_3O_4 were observed on the surface of Co_3O_4/Ti at different magnifications, confirming its deposition on the Ti mesh. SEM-EDS elemental mapping of a surface region of the Co_3O_4/Ti cathode (**Figure 3**) gave a value of 26.26 atom% for Co, indicating that the element was successfully deposited on the titanium mesh.

Figure 4 shows the XRD patterns of the calcined Co_3O_4/Ti electrode and their comparison with the reference powder patterns of cubic phase Co_3O_4 (PDF#42–1467) and Ti (PDF#44–1294). The characteristic peaks observed at 2θ of 35.1°, 38.4°, 40.2°, 53.0°, 62.9°, 70.7°, 76.2°, and 77.4° correspond to (100), (002), (101), (102), (110), (103), (112), and (201) planes of Ti (PDF#44–1294), respectively (**Figure 4A**). Inspection of the enlarged pattern obtained from the Co_3O_4/Ti cathode (**Figure 4B**) showed that the main peaks of Co_3O_4 at 2θ=31.3°, 36.9°, 44.8°, 59.4°, 65.2°, and 74.1°, correspond to the (220), (311), (400), (511), (440), and (620) planes of Co_3O_4, respectively. These results were in good agreement with the standard cubic phase (PDF#42–1467).

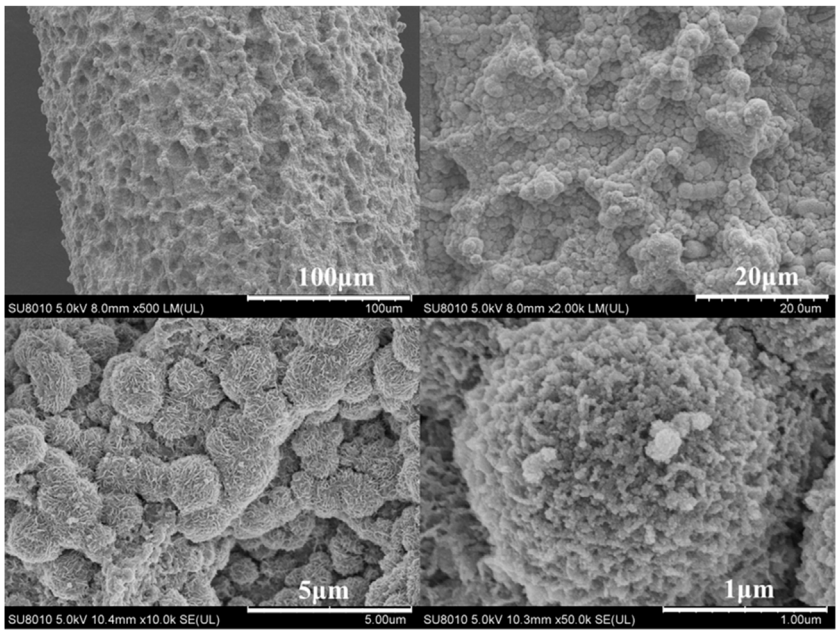

FIGURE 2 | SEM image of Co_3O_4/Ti at different resolutions.

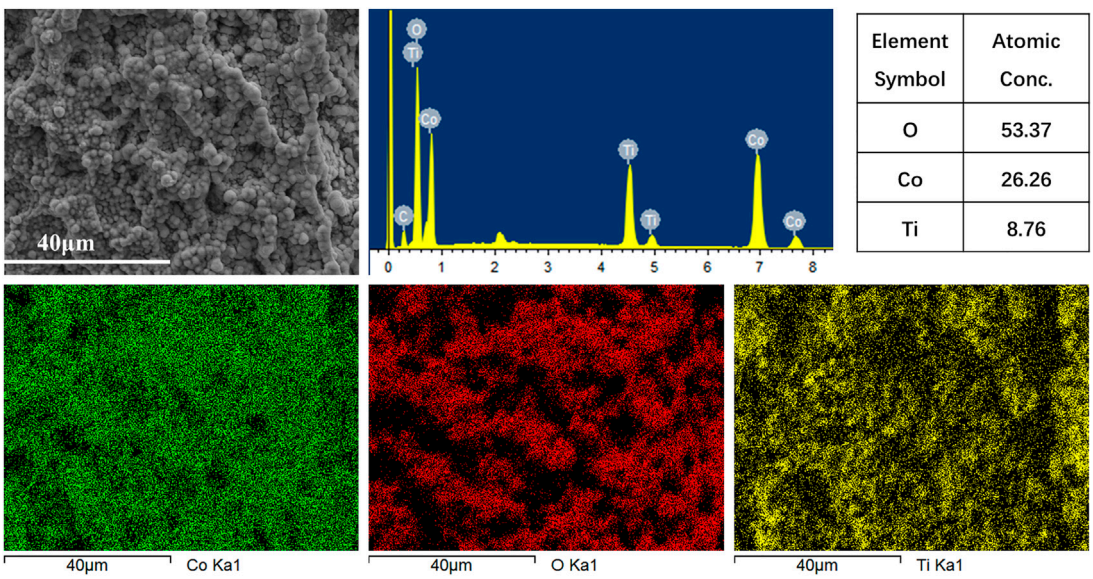

Element Symbol	Atomic Conc.
O	53.37
Co	26.26
Ti	8.76

FIGURE 3 | EDS elemental analysis of the surface of Co_3O_4/Ti cathode.

LSV was used to evaluate the electrocatalytic performance of the catalysts toward NO_3^--RR. **Figure 5A** shows the LSV curves obtained with Co_3O_4/Ti and Ti in the presence of NO_3^--N. The onset potential for NO_3^--RR using the Co_3O_4/Ti cathode (-0.7 V) was more positive than that using the Ti mesh (-1.0 V), indicating the improved performance with the composite catalyst. From −0.7 to −1.6 V, Co_3O_4/Ti gave a larger current response at all potentials due to its higher activity toward the NO_3^--RR compared with the Ti mesh. **Figure 5B** shows the effects of increasing NO_3^--N (0–500 mg/L) using Co_3O_4/Ti as the cathode. In the absence of NO_3^--N, the onset potential (i.e., for the electrolysis of water to produce H_2) was −0.9 V. The addition of NO_3^- produced a positive shift in the onset potential, and the corresponding current increased with increasing initial NO_3^--N due to the enhanced reduction reaction activity.

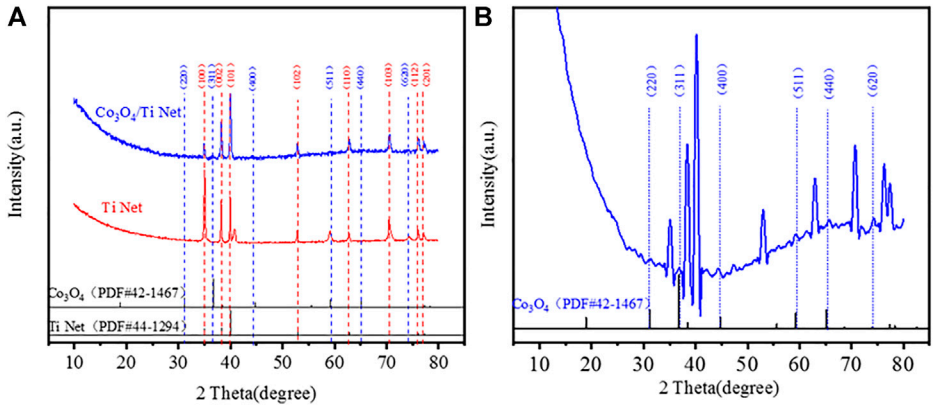

FIGURE 4 | Crystal structure of Co_3O_4/Ti cathode and comparison with the reference XRD powder patterns: **(A)** XRD patterns of Ti and Co_3O_4/Ti cathodes; **(B)** enlarged XRD patterns of Co_3O_4/Ti cathode.

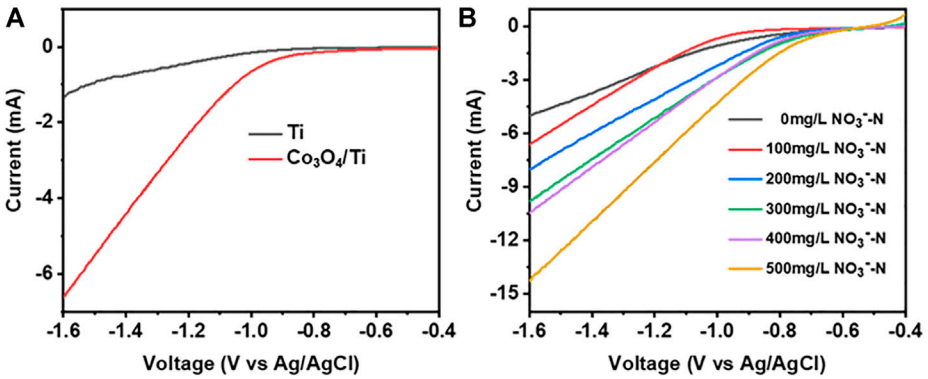

FIGURE 5 | LSV curves illustrating the NO_3^--N removal performance of the catalysts (0.1 M Na_2SO_4, 10 mV/s). **(A)** Effects of different catalysts at constant initial NO_3^--N concentration (100 mg/L). **(B)** Effects of increasing initial NO_3^--N concentrations using the Co_3O_4/Ti cathode.

3.2 Effects of Electrochemical Reaction Parameters on NO_3^--RR Using the Co_3O_4/Ti Cathode

3.2.1 Catalytic Activity of the Co_3O_4/Ti Cathode

To determine the effect of Co_3O_4 on NO_3^-RR activity, the NO_3^--N (100 mg/L) removal efficiencies of the Co_3O_4/Ti and Ti mesh cathodes were compared at a current density of 15 mA/cm^2 with a Pt plate as the anode (**Figure 6**). The results showed that the Co_3O_4/Ti cathode could achieve a NO_3^--N removal efficiency of ~98% in 2 h, compared with 6.4% using the Ti mesh, demonstrating the important role of Co_3O_4 in improving the performance of NO_3^--RR.

3.2.2 Effects of Current Density

Figure 7A,B show the rate of NO_3^--N removal using the Co_3O_4/Ti cathode and the corresponding fit of the experimental data to first-order kinetics. The increased removal efficiency with increasing current density over 5–15 mA/cm^2 could be attributed to enhanced electron transfer on the electrode surface of Co_3O_4/Ti, which increased the rate of NO_3^--RR. However, when the current density was increased from 15 to 20 mA/cm^2, the removal efficiency of NO_3^--N did not improve significantly. At higher current densities, the competing hydrogen evolution reaction consumes the extra charge, and the NO_3^--N removal efficiency decreases. **Figure 7C** shows that there was good correspondence between the reduction of NO_3^--N and the generation of NH_4^+-N. The reduction products were NH_4^+-N and N_2, while NO_2^--N was not detected (**Figure 7D**).

3.2.3 Effect of Initial NO_3^--N Concentration

The effects of initial NO_3^-N concentration on its removal efficiency using the Co_3O_4/Ti cathode and the generation of reduction products are shown in **Figure 8**. At initial NO_3^--N concentrations of <100 mg/L, the removal efficiency of the system was close to 100% at 2 h; and the corresponding reduction products were NH_4^+-N (60%) and N_2. At an initial NO_3^--N concentration of 200 mg/L, the removal efficiency decreased to ~58%, while the NH_4^+-N generation efficiency increased to ~79%. Under this condition, the higher

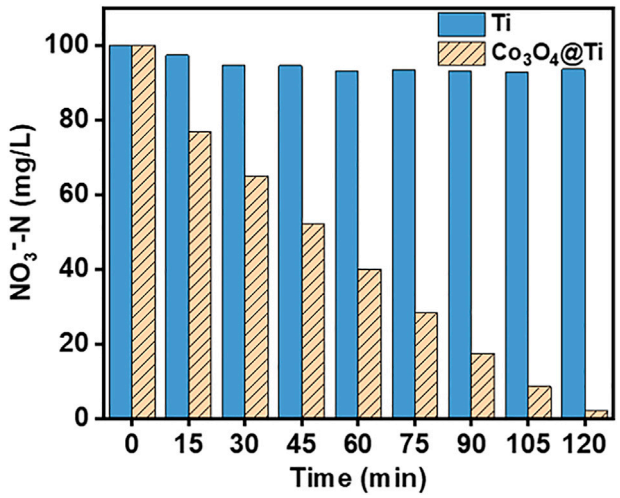

FIGURE 6 | Removal efficiencies of NO_3^--N by the Ti and Co_3O_4/Ti cathodes (Pt anode; [NO_3^--N], 100 mg/L, 150 ml; current density, 15 mA/cm^2; pH, 7.0; reaction time, 2 h).

initial NO_3^--N concentration suppressed the competing hydrogen evolution reaction, thus reducing its charge consumption at the electrode.

3.3 Effects of Cl^-

The main product of electrocatalytic NO_3^- reduction is NH_4^+, which is also a contaminant requiring removal. However, in the presence of Cl^-, which is widely present in drinking water and industrial water, the active species participating in the oxidative transformation of NH_4^+-N to N_2 at the anode (**Eqs 6–9**) will increase TN removal. The IrO_2-RuO_2/Ti electrode is widely employed in the chlor-alkali industry because of its high chlorine evolution performance. To investigate the effects of Cl^- on NH_4^+-N generation and NO_3^--N removal, various concentrations of Cl^- were presented to a Co_3O_4/Ti/IrO_2-RuO_2/Ti NO_3^--N removal system (**Table 1**). As the concentration of Cl^- increased from 0 to 2000 mg/L, the removal efficiencies of NO_3^--N were all >90%. At 4,000 mg/L Cl^-, the removal efficiency decreased to 83.99% due to the oxidation of NH_4^+ to NO_3^- by HClO/ClO^-. The increase in Cl^- concentration increased the amount of HClO/ClO^- generated by anodic oxidation to reduce NH_4^+-N to N_2. Hence, NH_4^+-N generation decreased and TN removal efficiency increased with increasing Cl^- concentration. The TN removal efficiency reached 78.1% with negligible NH_4^+-N generation (0.34%) and without NO_2^--N accumulation.

3.4 Long-Term Stability

In addition to the initial activity, the long-term performance of a catalyst is an essential requirement for its commercial application.

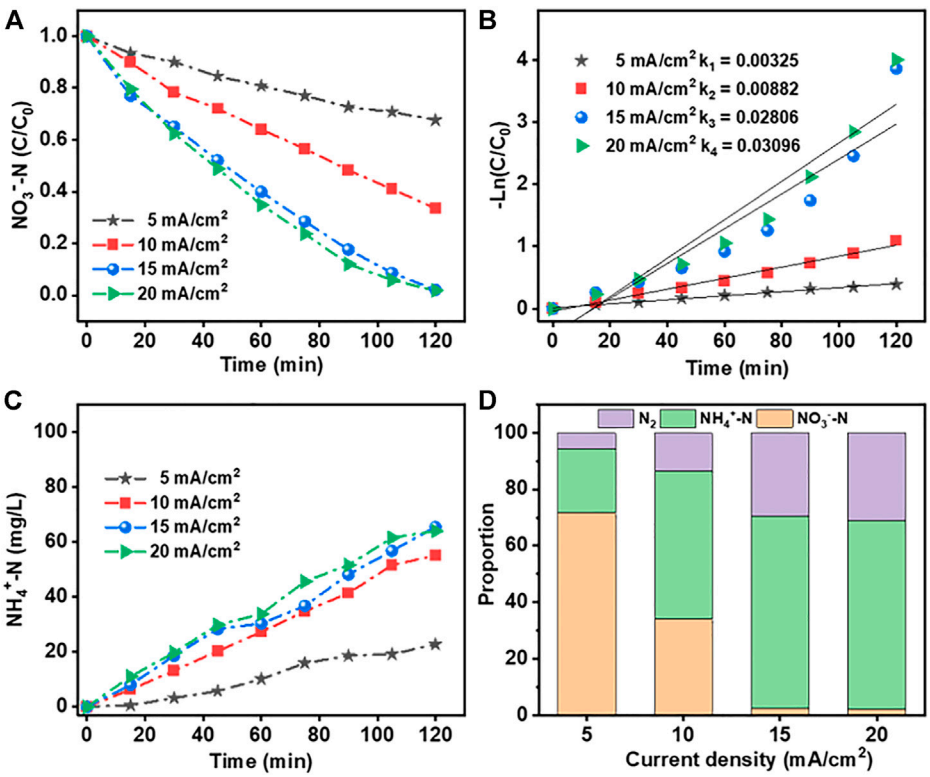

FIGURE 7 | Effects of current density on the NO_3^--RR using the Co_3O_4/Ti cathode (Pt anode; [NO_3^--N], 100 mg/L, 150 ml; initial pH, 7.0; reaction time, 2 h): **(A)** and **(B)** rate of loss of NO_3^--N and the fit of the data to first-order kinetics; **(C)** rate of generation of NH_4^+-N; and **(D)** distribution of the products formed.

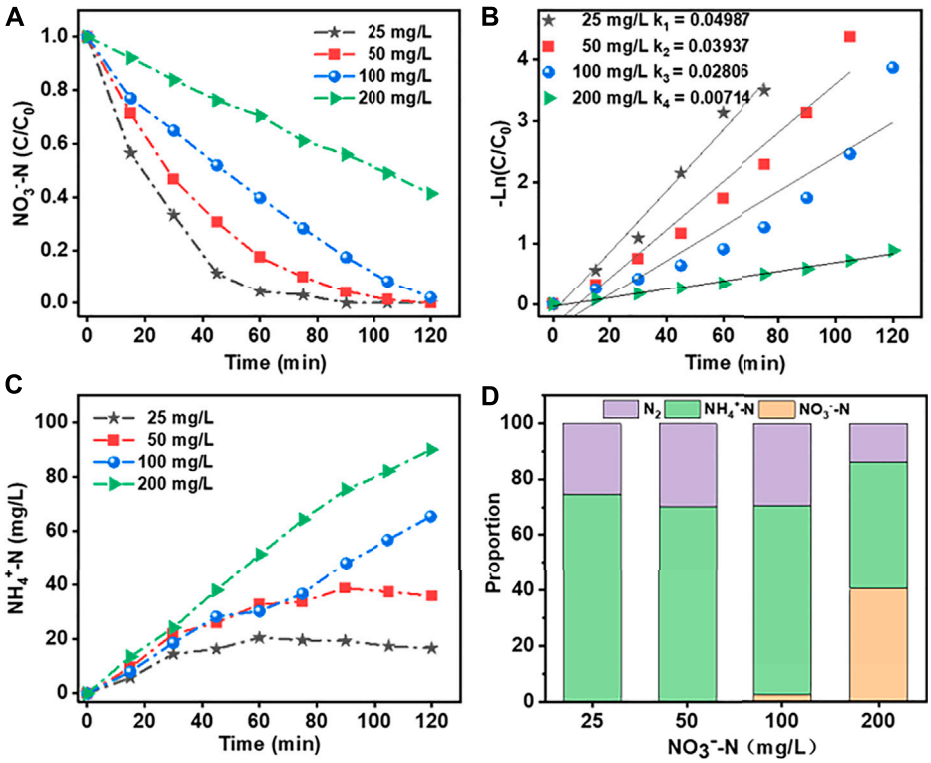

FIGURE 8 | Effects of different initial NO_3^--N concentrations on NO_3^--RR using the Co_3O_4/Ti cathode (Pt anode; reaction solution, 150 ml; current density, 15 mA/cm^2; initial pH, 7.0; reaction time, 2 h): **(A)** and **(B)** Rate of loss of NO_3^--N and the fit of the data to first-order kinetics; **(C)** generation of NH_4^+-N; and **(D)** product distributions.

TABLE 1 | Effects of Cl^- on the Co_3O_4/Ti/IrO_2-RuO_2/Ti NO_3^--N removal system.

Cl^- Concentration (mg/L)	NO_3^--N removal (%)	NO_2^--N generation (%)	NH_4^+-N generation (%)	TN removal (%)
0	92.2	—	54.5	24.8
1000	90.7	—	37.2	38.3
2000	91.1	—	19.9	60.3
4,000	84.0	—	0.340	78.1

Figure 9 shows the changes in NO_3^--N removal and distribution of generated products over 4 h, and 10 consecutive cycles of 2 h each, using the system. At an initial concentration of 100 mg/L, almost all NO_3^--N is converted into N_2 after 4 h (**Figure 9A**). After 10 cycles (**Figure 9B**), the removal efficiencies of NO_3^--N (~90%) and TN remained unchanged.

3.5 EC and CE

EC and CE are key evaluation factors for the commercial electrochemical treatment process (Zeng et al., 2020). The EC and CE under different process conditions using the system were calculated. It can be seen from **Figure 10A,B** that within 1 h after the start of the reaction, EC is lower and CE is higher than those of the follow-up experiments, but the NO_3^--N removal rate is only 58.52%. After 2 h, the NO_3^--N removal efficiency reaches 93.39% with an EC of 0.10 kW h/g NO_3^--N and a CE of 40.3%. There was no significant improvement in the follow-up, but the EC continued to rise, and the CE continued to decline.

The effect of the initial NO_3^--N concentration is demonstrated in **Figures 10C,D**. As the NO_3^--N concentration increased, the EC decreased and CE increased. This can be explained by the increase in the contact area between NO_3^--N and the electrode surface with increasing concentrations, which promotes the reduction reaction. From an economic viewpoint, the results indicate that the Co_3O_4/Ti/IrO_2-RuO_2/Ti electrocatalytic process is more suitable for wastewater with high concentrations of NO_3^-. The small amount of NO_3^- remaining in the electrochemically treated wastewater can be removed by other processes, such as the electrocatalytic removal of NO_3^--N, which can be combined with constructed wetlands for wastewater control/remediation.

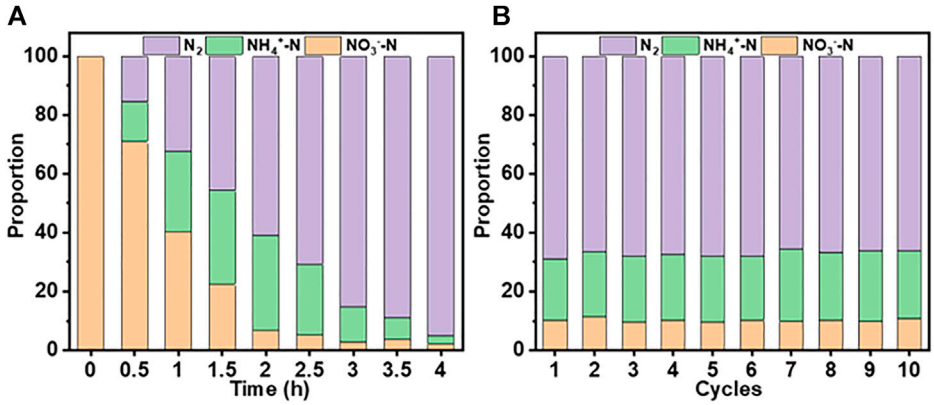

FIGURE 9 | Changes in NO_3^--N removal and the distribution of generated products for the Co_3O_4/Ti/IrO_2-RuO_2/Ti system ([NO_3^--N], 100 mg/L, 150 ml; current density, 15 mA/cm^2; pH, 7.0; cycle time, 2 h). **(A)** Changes over 4 h. **(B)** Changes over 10 cycles.

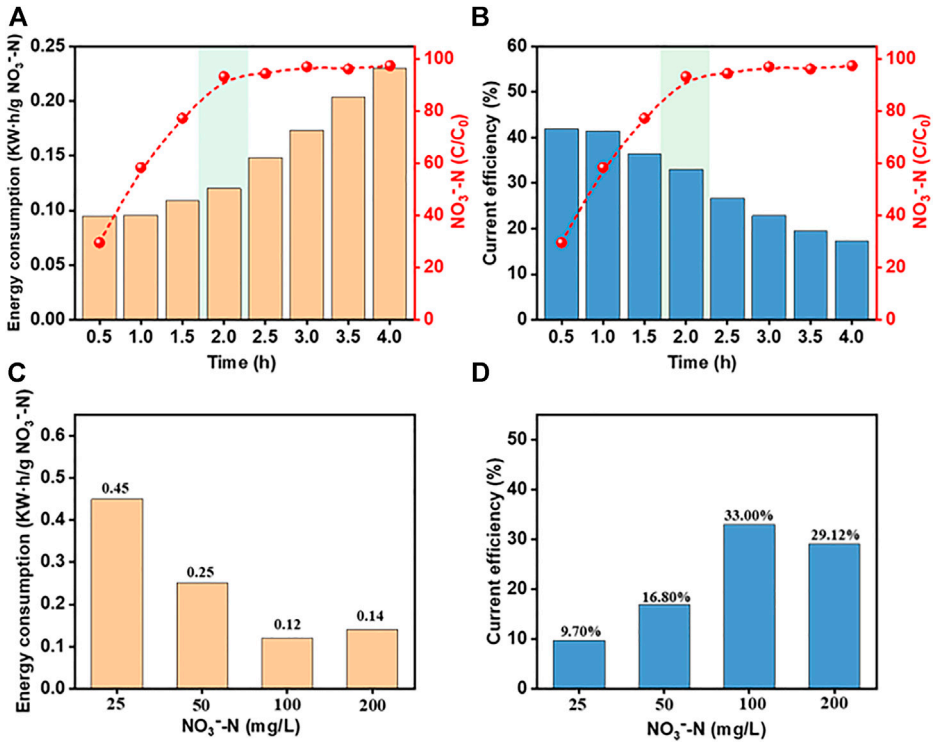

FIGURE 10 | Effects of reaction time and initial NO_3^--N concentrations on the operational efficiency. **(A)** and **(C)** EC; **(B)** and **(D)** CE (pH, 7.0; current density, 15 mA/cm^2; [Cl^-], 2000 mg/L; reaction time, 2 h).

4 CONCLUSION

A Co_3O_4/Ti electrode was successfully prepared by electrodeposition, and the material showed good electrocatalytic performance toward NO_3^--RR. At an initial concentration of 100 mg/L NO_3^--N, the removal rate was ~98% in 2 h (Pt anode; pH, 7.0; current density, 15 mA/cm^2). The corresponding generation of NH_4^+-N was ~60%, while NO_2^--N was not detected. When IrO_2-RuO_2/Ti was employed as the anode in the presence of Cl^- (2000 mg/L), the removal efficiencies for NO_3^--N and TN under the same operating conditions were ~91% and ~60%, respectively, with an EC of 0.10 kW h/g NO_3^--N and a CE of 40.3%. After 4 h of continuous operation, 100% of NO_3^--N was converted into N_2. In addition, the system could maintain the removal

efficiencies of ~90% and ~60% for NO_3^--N and TN, respectively, after 10 consecutive cycles (2 h each). This work provides a simple preparation method of electrodeposited Co_3O_4/Ti with good catalytic performance and stability, which provides a new preparation strategy for the Co_3O_4 catalytic electrode.

DATA AVAILABILITY STATEMENT

The original contributions presented in the study are included in the article/Supplementary Material, further inquiries can be directed to the corresponding author.

AUTHOR CONTRIBUTIONS

CW: conceptualization, methodology, data analysis, and writing—original draft. ZC: data curation. HH: validation. HL: resources and funding acquisition. SW: conceptualization, investigation, and writing—review and editing.

FUNDING

This work was supported by the National Natural Science Foundation of China (grant numbers 51978181, 51808527, 51727812, and 52131003).

REFERENCES

Barakat, A., Mouhtarim, G., Saji, R., and Touhami, F. (2020). Health Risk Assessment of Nitrates in the Groundwater of Beni Amir Irrigated Perimeter, Tadla Plain, Morocco. *Hum. Ecol. Risk Assess. Int. J.* 26 (7), 1864–1878. doi:10.1080/10807039.2019.1613631

Chen, J., Shi, H., and Lu, J. (2007). Electrochemical Treatment of Ammonia in Wastewater by RuO2-IrO2-TiO2/Ti Electrodes. *J. Appl. Electrochem* 37 (10), 1137–1144. doi:10.1007/s10800-007-9373-6

Clauwaert, P., Rabaey, K., Aelterman, P., De Schamphelaire, L., Pham, T. H., Boeckx, P., et al. (2007). Biological Denitrification in Microbial Fuel Cells. *Environ. Sci. Technol.* 41 (9), 3354–3360. doi:10.1021/es062580r

Della Rocca, C., Belgiorno Vand Meriç, S. (2007). Overview of *In-Situ* Applicable Nitrate Removal Processes. *Desalination J.* 204 (1), 46–62. doi:10.1016/j.desal.2006.04.023

Elmidaoui, A., Elhannouni, F., Menkouchi Sahli, M. A., Chay, L., Elabbassi, H., Hafsi, M., et al. (2001). Pollution of Nitrate in Moroccan Ground Water: Removal by Electrodialysis. *Desalination J.* 136 (1), 325–332. doi:10.1016/s0011-9164(01)00195-3

Garcia-Segura, S., Lanzarini-Lopes, M., Hristovski, K., and Westerhoff, P. (2018). Electrocatalytic Reduction of Nitrate: Fundamentals to Full-Scale Water Treatment Applications. *Appl. Catal. B Environ.* 236, 546–568. doi:10.1016/j.apcatb.2018.05.041

Gayen, P., Spataro, J., Avasarala, S., Ali, A.-M., Cerrato, J. M., and Chaplin, B. P. (2018). Electrocatalytic Reduction of Nitrate Using Magnéli Phase TiO2 Reactive Electrochemical Membranes Doped with Pd-Based Catalysts. *Environ. Sci. Technol.* 52 (16), 9370–9379. doi:10.1021/acs.est.8b03038

Jasper, J. T., Jones, Z. L., Sharp, J. O., and Sedlak, D. L. (2014). Nitrate Removal in Shallow, Open-Water Treatment Wetlands. *Environ. Sci. Technol.* 48 (19), 11512–11520. doi:10.1021/es502785t

Kapoor, A., and Viraraghavan, T. (1997). Nitrate Removal from Drinking Water-Review. *J. Environ. Eng.* 123 (4), 371–380. doi:10.1061/(asce)0733-9372(1997)123:4(371)

Khalil, A. M. E., Eljamal, O., Jribi, S., and Matsunaga, N. (2016). Promoting Nitrate Reduction Kinetics by Nanoscale Zero Valent Iron in Water via Copper Salt Addition. *Chem. Eng. J.* 287, 367–380. doi:10.1016/j.cej.2015.11.038

Kubicz, J., Pawełczyk, A., and Lochyński, P. (2018). Environmental Health Risk Posed by Contamination of the Individual Water Wells. *Chemosphere* 208, 247–256. doi:10.1016/j.chemosphere.2018.05.182

Serio, F., Miglietta, P. P., Lamastra, L., Ficocelli, S., Intini, F., De Leo, F., et al. (2018). Groundwater Nitrate Contamination and Agricultural Land Use: A Grey Water Footprint Perspective in Southern Apulia Region (Italy). *Sci. Total Environ.* 645, 1425–1431. doi:10.1016/j.scitotenv.2018.07.241

Soto-Hernández, J., Santiago-Ramirez, C. R., Ramirez-Meneses, E., Luna-Trujillo, M., Wang, J-A., Lartundo-Rojas, L., et al. (2019). Electrochemical Reduction of NOx Species at the Interface of Nanostructured Pd and PdCu Catalysts in Alkaline Conditions. *Appl. Catal. B Environ. J.* 259, 118048.

Spalding, R. F., and Exner, M. E. (1993). Occurrence of Nitrate in Groundwater-A Review. *J. Environ. Qual.* 22 (3), 392–402. doi:10.2134/jeq1993.00472425002200030002x

Su, L., Li, K., Zhang, H., Fan, M., Ying, D., Sun, T., et al. (2017). Electrochemical Nitrate Reduction by Using a Novel Co 3 O 4/Ti Cathode. *Water Res.* 120, 1–11. doi:10.1016/j.watres.2017.04.069

Taguchi, S., and Feliu, J. M. (2007). Electrochemical Reduction of Nitrate on Pt(S)[n(111)×(111)] Electrodes in Perchloric Acid Solution. *Electrochimica Acta* 52 (19), 6023–6033. doi:10.1016/j.electacta.2007.03.057

Teng, W., Bai, N., Liu, Y., Liu, Y., Fan, J., and Zhang, W.-x. (2018). Selective Nitrate Reduction to Dinitrogen by Electrocatalysis on Nanoscale Iron Encapsulated in Mesoporous Carbon. *Environ. Sci. Technol.* 52 (1), 230–236. doi:10.1021/acs.est.7b04775

Yang, G. C. C., and Lee, H.-L. (2005). Chemical Reduction of Nitrate by Nanosized Iron: Kinetics and Pathways. *Water Res.* 39 (5), 884–894. doi:10.1016/j.watres.2004.11.030

Yang, J., Sebastian, P., Duca, M., Hoogenboom, T., and Koper, M. T. M. (2014). pH Dependence of the Electroreduction of Nitrate on Rh and Pt Polycrystalline Electrodes. *Chem. Commun.* 50 (17), 2148–2151. doi:10.1039/c3cc49224a

Yang, M., Wang, J., Shuang, C., and Li, A. (2020). The Improvement on Total Nitrogen Removal in Nitrate Reduction by Using a Prepared CuO-Co3O4/Ti Cathode. *Chemosphere* 255, 126970. doi:10.1016/j.chemosphere.2020.126970

Yi, Z., Kangning, C., Wei, W., Wang, J., and Lee, S. (2007). Effect of IrO2 Loading on RuO2-IrO2-TiO2 Anodes: A Study of Microstructure and Working Life for the Chlorine Evolution Reaction. *Ceram. Int.* 33 (6), 1087–1091. doi:10.1016/j.ceramint.2006.03.025

Zeng, Y., Priest, C., Wang, G., and Wu, G. (2020). Restoring the Nitrogen Cycle by Electrochemical Reduction of Nitrate: Progress and Prospects. *Small Methods* 4, 2000672. doi:10.1002/smtd.202000672

Zhang, X., Wang, Y., Liu, C., Yu, Y., Lu, S., and Zhang, B. (2021). Recent Advances in Non-Noble Metal Electrocatalysts for Nitrate Reduction. *Chem. Eng. J.* 403, 126269. doi:10.1016/j.cej.2020.126269

Zhang, Z., Xu, Y., Shi, W., Wang, W., Zhang, R., Bao, X., et al. (2016). Electrochemical-catalytic Reduction of Nitrate over Pd-Cu/γAl 2 O 3 Catalyst in Cathode Chamber: Enhanced Removal Efficiency and N 2 Selectivity. *Chem. Eng. J.* 290, 201–208. doi:10.1016/j.cej.2016.01.063

Conflict of Interest: The authors declare that the research was conducted in the absence of any commercial or financial relationships that could be construed as a potential conflict of interest.

Publisher's Note: All claims expressed in this article are solely those of the authors and do not necessarily represent those of their affiliated organizations, or those of the publisher, the editors, and the reviewers. Any product that may be evaluated in this article, or claim that may be made by its manufacturer, is not guaranteed or endorsed by the publisher.